Time-Variant Reliability Analysis of Linear Elastic Systems Subjected to Fully Nonstationary Stochastic Excitations

Michele Barbato, M.ASCE[1]; and Joel P. Conte, M.ASCE[2]

Abstract: This paper presents closed-form solutions for the nongeometric spectral characteristics of nonstationary stochastic processes representing the response of linear elastic structural models subjected to fully nonstationary excitation processes. These spectral characteristics provide a complete description of the nonstationary stochastic processes representing the dynamic response of linear structural models when the input excitation is a Gaussian process. In particular, the nongeometric spectral characteristics can be used to evaluate the time-variant central frequency and bandwidth parameters of nonstationary stochastic processes. The closed-form solutions derived in this paper are used to evaluate the time-variant statistics and the first-passage probability of the response of single-degree-of-freedom and multidegree-of-freedom linear elastic structural models subjected to a well-known, fully nonstationary earthquake ground motion model. The new analytical results presented in this paper can be used in a number of structural dynamic applications. **DOI: 10.1061/(ASCE)EM.1943-7889.0000895.**

Author keywords: Random process; Nonstationarity; Spectral characteristics; Bandwidth parameter; Central frequency; Earthquake ground motion; Classical and nonclassical damping.

Introduction

In general, the dynamic response behavior of structural and mechanical systems subjected to uncertain dynamic excitations can be described using random processes. The probabilistic characterization of these random processes can be extremely complex when nonstationary and/or non-Gaussian input processes are involved. In specific applications, an incomplete description of the stochastic processes representing the structural dynamic response may suffice (e.g., a description based on the spectral characteristics of the processes under study) (Priestley 1987). For stationary stochastic processes, the spectral characteristics are defined as the geometric spectral moments of the power spectral density (PSD) function of the process (Priestley 1987). By contrast, the so-called nongeometric spectral characteristics (NGSCs) (Di Paola 1985; Michaelov et al. 1999; Barbato and Conte 2008; Barbato and Vasta 2010) can be used to evaluate the time-variant central frequency and bandwidth parameters, which characterize a nonstationary stochastic process in a synthetic way. The NGSCs have been proven appropriate for describing nonstationary stochastic processes and can be effectively used in structural reliability applications, such as the computation of the time-variant probability of a random process out-crossing a specified limit-state threshold (Corotis et al. 1972).

In this paper, using the definition of NGSCs for general complex-valued nonstationary stochastic processes proposed in Barbato and Conte (2008) and complex modal analysis, closed-form solutions for the NGSCs of nonstationary stochastic processes representing the displacement, velocity, and/or acceleration response of linear elastic structural models subjected to fully nonstationary (both in amplitude and frequency) stochastic excitations are obtained. It is noteworthy that, whereas closed-form solutions have been available for more than 2 decades for the simpler case of geometric spectral moments of stationary stochastic processes (Spanos 1983; Spanos and Miller 1994), the availability of closed-form solutions for the NGSCs of nonstationary response processes of linear systems is very recent for the case of time-modulated white noise (Barbato and Conte 2008) and colored noise excitation processes (Barbato and Vasta 2010).

Here, the results presented in Barbato and Vasta (2010) are extended to more general time-modulating and PSD functions. The NGSCs are used in this study to derive exactly and in closed form the time-variant statistics (including variance of the displacement and velocity responses, cross-correlation between displacement and velocity responses, and central frequency and bandwidth parameter of the displacement responses) of the response processes of single-degree-of-freedom (SDOF) and both classically and nonclassically damped multidegree-of-freedom (MDOF) linear elastic systems subjected to nonstationary excitation from at-rest initial conditions. These closed-form response statistics are then used to estimate, using existing analytical approximations (Crandall 1970; Vanmarcke 1975; Barbato and Conte 2011), the first-passage failure probability of SDOF and MDOF linear models of structures subjected to nonstationary seismic excitations. For the sake of simplicity and without loss of generality, all random processes considered in this study are zero-mean processes. For these processes, the autocovariance and cross-covariance functions coincide with their autocorrelation and cross-correlation functions, respectively.

Spectral Characteristics of Nonstationary Random Processes

A nonstationary stochastic process $X(t)$ can be expressed in the general form of a Fourier-Stieltjes integral as (Priestley 1965, 1987; Shinozuka 1970)

[1]Associate Professor, Dept. of Civil and Environmental Engineering, Louisiana State Univ. and A&M College, 3418H Patrick F. Taylor Hall, Nicholson Extension, Baton Rouge, LA 70803. E-mail: mbarbato@lsu.edu

[2]Professor, Dept. of Structural Engineering, Univ. of California at San Diego, 9500 Gilman Dr., La Jolla, CA 92093-0085 (corresponding author). E-mail: jpconte@ucsd.edu

Note. This manuscript was submitted on December 20, 2013; approved on October 15, 2014; published online on November 20, 2014. Discussion period open until April 20, 2015; separate discussions must be submitted for individual papers. This paper is part of the ***Journal of Engineering Mechanics***, © ASCE, ISSN 0733-9399/04014173(10)/$25.00.

$$X(t) = \int_{-\infty}^{\infty} A_X(\omega, t) \cdot e^{j\cdot\omega\cdot t} \cdot \mathrm{d}Z(\omega) \tag{1}$$

in which t = time; ω = frequency parameter; $j = \sqrt{-1}$; $A_X(\omega, t)$ = complex-valued deterministic time-frequency modulating function; and $\mathrm{d}Z(\omega)$ = zero-mean orthogonal-increment process (Priestley 1987). The process $X(t)$ has the following evolutionary PSD function:

$$\Phi_{XX}(\omega, t) = A_X^*(\omega, t) \cdot \Phi_{X_S X_S}(\omega) \cdot A_X(\omega, t) \tag{2}$$

in which $\Phi_{X_S X_S}(\omega)$ = PSD function of the embedded stationary process $X_S(t) = \int_{-\infty}^{\infty} e^{j\cdot\omega\cdot t} \cdot \mathrm{d}Z(\omega)$; and superscript $(\ldots)^*$ = complex-conjugate operator.

It is also convenient to define the auxiliary process $Y(t)$ as the modulation [with modulating function $A_X(\omega, t)$] of the stationary process $Y_S(t)$, which is defined as the Hilbert transform of the embedded stationary process $X_S(t)$ (Arens 1957; Dugundji 1958)

$$Y(t) = -j \cdot \int_{-\infty}^{\infty} \mathrm{sgn}(\omega) \cdot A_X(\omega, t) \cdot e^{j\cdot\omega\cdot t} \cdot \mathrm{d}Z(\omega) \tag{3}$$

in which $\mathrm{sgn}(\ldots)$ = sign function. For each nonstationary stochastic process $X(t)$, two sets of NGSCs can be defined as (Barbato and Conte 2008)

$$\begin{aligned} c_{ik,XX}(t) &= \int_{-\infty}^{\infty} \Phi_{X^{(i)}X^{(k)}}(\omega, t) \cdot \mathrm{d}\omega = \sigma_{X^{(i)}X^{(k)}}(t) \\ c_{ik,XY}(t) &= \int_{-\infty}^{\infty} \Phi_{X^{(i)}Y^{(k)}}(\omega, t) \cdot \mathrm{d}\omega = \sigma_{X^{(i)}Y^{(k)}}(t) \end{aligned} \tag{4}$$

where $\sigma_{X^{(i)}X^{(k)}}(t)$ = cross-covariance of random processes $X^{(i)}(t)$ and $X^{(k)}(t)$ (at the same time t); and $\sigma_{X^{(i)}Y^{(k)}}(t)$ = cross-covariance of random processes $X^{(i)}(t)$ and $Y^{(k)}(t)$ (at the same time t), in which

$$W^{(m)}(t) = \frac{\mathrm{d}^m W(t)}{\mathrm{d}t^m}; \quad W = X, Y; \quad m = i, k \tag{5}$$

The evolutionary cross-PSD functions $\Phi_{X^{(i)}W^{(k)}}(\omega, t)$ ($W = X, Y$ and $i, k = 0, 1, \ldots$) are given by

$$\Phi_{X^{(i)}W^{(k)}}(\omega, t) = A_{X^{(i)}}^*(\omega, t) \cdot \Phi_{X_S X_S}(\omega) \cdot A_{W^{(k)}}(\omega, t) \tag{6}$$

where (Peng and Conte 1998)

$$A_{W^{(i)}}(\omega, t) = e^{-j\cdot\omega\cdot t} \cdot \frac{\partial^i}{\partial t^i}\left[A_W(\omega, t) \cdot e^{j\cdot\omega\cdot t}\right] \tag{7}$$

Herein, it is assumed that the time derivative processes involved in Eq. (5) exist in the mean-square sense. In the particular case when $i = k = n$, the cross-covariance in the first line of Eq. (4) reduces to the variance of the nth time derivative of the process $X(t)$ [i.e., $\sigma_{X^{(n)}X^{(n)}}(t) = \sigma^2_{X^{(n)}}(t)$].

The four NGSCs $c_{00,XX}(t)$, $c_{11,XX}(t)$, $c_{01,XX}(t)$, and $c_{01,XY}(t)$ are particularly relevant to random vibration theory and time-variant reliability analysis. In fact, $c_{00,XX}(t)$ and $c_{11,XX}(t)$ = variance of process $X(t)$ and its first time derivative [i.e., $\sigma^2_X(t)$ and $\sigma^2_{\dot{X}}(t)$, where superposed dot = differentiation with respect to time], respectively; $c_{01,XX}(t)$ = cross-covariance of process $X(t)$ and its first time derivative [i.e., $\sigma_{X\dot{X}}(t)$]; and $c_{01,XY}(t)$ = cross-covariance of process $X(t)$ and the first time derivative of process $Y(t)$ [i.e., $\sigma_{X\dot{Y}}(t)$]. The definitions in Eq. (4) for $c_{00,XX}(t)$, $c_{11,XX}(t)$, $c_{01,XX}(t)$, and $c_{01,XY}(t)$ are valid for both real-valued and complex-valued nonstationary stochastic processes (Barbato and Conte 2008). In the case of real-valued nonstationary stochastic processes, these definitions are equivalent to those proposed by Di Paola (1985) and Michaelov et al. (1999). The NGSCs $c_{00,XX}(t)$, $c_{11,XX}(t)$, and $c_{01,XY}(t)$ are used in the definition of the time-variant central frequency, $\omega_c(t)$, and bandwidth parameter, $q(t)$, of the nonstationary stochastic process $X(t)$ as (Barbato and Conte 2008)

$$\omega_c(t) = \frac{c_{01,XY}(t)}{c_{00,XX}(t)} \tag{8}$$

$$q(t) = \left[1 - \frac{c^2_{01,XY}(t)}{c_{00,XX}(t) \cdot c_{11,XX}(t)}\right]^{1/2} \tag{9}$$

The time-variant central frequency and bandwidth parameter are useful in describing the time-variant spectral properties of a real-valued nonstationary stochastic process $X(t)$. The central frequency $\omega_c(t)$ provides a measure of the average frequency of the process at each instant of time. The bandwidth parameter $q(t)$ provides information on the spectral bandwidth of the process at each instant of time (it is close to 1 for a narrowband process and decreases as the bandwidth increases). A nonstationary stochastic process can behave as a narrowband and a broadband process at different instants of time. The computation of the central frequency and bandwidth parameter defined in Eqs. (8) and (9) for complex-valued nonstationary stochastic processes is needed for the solution of problems requiring a state-space representation (e.g., in the presence of nonclassical damping). In addition, the bandwidth parameter $q(t)$ is an essential ingredient of analytical approximations of the time-variant failure probability for a first-passage reliability problem (Rice 1944, 1945; Lin 1967; Crandall 1970; Corotis et al. 1972; Vanmarcke 1975; Barbato and Conte 2011; Ghazizadeh et al. 2012).

Spectral Characteristics of the Stochastic Response of Linear Systems Subjected to Fully Nonstationary Excitations

Complex Modal Analysis

A state-space formulation of the equations of motion for a linear MDOF system is useful to describe the response of both classically and nonclassically damped systems (Reid 1983). The general (second-order) equations of motion for an n-degree-of-freedom (DOF) linear system are, in matrix form

$$\mathbf{M} \cdot \ddot{\mathbf{U}}(t) + \mathbf{C} \cdot \dot{\mathbf{U}}(t) + \mathbf{K} \cdot \mathbf{U}(t) = \mathbf{P} \cdot F(t) \tag{10}$$

in which $\mathbf{M}$, $\mathbf{C}$, and $\mathbf{K} = n \times n$ time-invariant mass, damping, and stiffness matrices, respectively; $\mathbf{U}(t)$ = length-n vector of nodal displacements; $\mathbf{P}$ = length-n load distribution vector; $F(t)$ = scalar function describing the time history of the external loading (random process); and a superposed dot denotes differentiation with respect to time. The matrix equation of motion given in Eq. (10) can be recast into the following first-order matrix equation:

$$\dot{\mathbf{Z}}(t) = \mathbf{G} \cdot \mathbf{Z}(t) + \tilde{\mathbf{P}} \cdot F(t) \tag{11}$$

where

$$\mathbf{Z}(t) = \begin{bmatrix} \mathbf{U}(t) \\ \dot{\mathbf{U}}(t) \end{bmatrix}_{(2n\times 1)}; \quad \mathbf{G} = \begin{bmatrix} \mathbf{0}_{n\times n} & \mathbf{I}_{n\times n} \\ -\mathbf{M}^{-1}\cdot\mathbf{K} & -\mathbf{M}^{-1}\cdot\mathbf{C} \end{bmatrix}_{(2n\times 2n)}; \quad \tilde{\mathbf{P}} = \begin{bmatrix} \mathbf{0}_{n\times 1} \\ \mathbf{M}^{-1}\cdot\mathbf{P} \end{bmatrix}_{(2n\times 1)} \tag{12}$$

The subscripts in Eq. (12) indicate the dimensions of the vectors and matrices to which they are attached. Using the complex modal matrix $\mathbf{T}$ formed by the complex eigenmodes of the system matrix $\mathbf{G}$, the first-order matrix equation of motion, Eq. (11), can be decoupled into the following $2n$ normalized complex modal equations:

$$\dot{S}_i(t) = \lambda_i \cdot S_i(t) + F(t); \quad i = 1, 2, \ldots, 2n \tag{13}$$

in which $\mathbf{S} = [S_1(t) S_2(t) \ldots S_{2n}(t)]^T$ = normalized complex modal response vector; λ_i ($i = 1, \ldots, 2n$) = complex eigenvalues of the system matrix $\mathbf{G}$; and the superscript $(\ldots)^T$ denotes the matrix transpose operator. The response of the linear MDOF system can be obtained as

$$\mathbf{Z}(t) = \tilde{\mathbf{T}} \cdot \mathbf{S}(t) \tag{14}$$

in which $\tilde{\mathbf{T}} = \mathbf{T} \cdot \mathbf{\Gamma}$ = effective modal participation matrix; $\mathbf{\Gamma}$ = diagonal matrix containing the $2n$ modal participation factors Γ_i, defined as the ith component of vector $\mathbf{T}^{-1} \cdot \tilde{\mathbf{P}} = [\Gamma_1 \Gamma_2 \ldots \Gamma_{2n}]^T$. Assuming that the system is initially at rest, the solution to Eq. (13) can be expressed as the Duhamel integral

$$S_i(t) = \int_0^t e^{\lambda_i \cdot (t-\tau)} \cdot F(\tau) \cdot \mathrm{d}\tau = \int_{-\infty}^{\infty} A_{S_i}(\omega, t) \cdot e^{j\cdot\omega\cdot t} \cdot \mathrm{d}Z(\omega); \quad i = 1, 2, \ldots, 2n \tag{15}$$

where (Peng and Conte 1998)

$$F(t) = \int_{-\infty}^{\infty} A_F(\omega, t) \cdot e^{j\cdot\omega\cdot t} \cdot \mathrm{d}Z(\omega) \tag{16}$$

$$A_{S_i}(\omega, t) = \int_{-\infty}^{t} e^{(\lambda_i - j\cdot\omega)\cdot(t-\tau)} \cdot A_F(\omega, \tau) \cdot \mathrm{d}\tau; \quad i = 1, 2, \ldots, 2n \tag{17}$$

The complex eigenvalues and eigenvectors of matrix $\mathbf{G}$, as well as the normalized complex modal responses, $S_i(t)$ ($i = 1, 2, \ldots, 2n$), are complex conjugates by pairs.

NGSCs of Response Processes of Linear MDOF Systems Using Complex Modal Analysis

The state-space formulation of the equations of motion is advantageous for the computation of the NGSCs of response processes for both classically and nonclassically damped linear MDOF systems. If the input processes are Gaussian, the response processes of linear elastic MDOF systems are also Gaussian. If $U_i(t)$ denotes the ith DOF displacement response process of a linear elastic MDOF system subjected to Gaussian excitation, the only spectral characteristics required for time-variant reliability analysis (related to or based on this DOF displacement response) are ($i = 1, 2, \ldots, n$)

$$\begin{aligned} c_{00,U_iU_i}(t) &= \sigma^2_{U_i}(t) \\ c_{11,U_iU_i}(t) &= \sigma^2_{\dot{U}_i}(t) \\ c_{01,U_iU_i}(t) &= \sigma_{U_i\dot{U}_i}(t) \\ c_{01,U_iV_i}(t) &= \sigma_{U_i\dot{V}_i}(t) \end{aligned} \tag{18}$$

where $\dot{V}_i$ = first time derivative of the auxiliary process V_i defined as [Eq. (3)]

$$V_i(t) = -j \cdot \int_{-\infty}^{\infty} \mathrm{sgn}(\omega) \cdot A_{U_i}(\omega, t) \cdot e^{j\cdot\omega\cdot t} \cdot \mathrm{d}Z(\omega); \quad i = 1, 2, \ldots, 2n \tag{19}$$

in which $A_{U_i}(\omega, t)$ = time-frequency modulating function of the process $U_i(t)$. The auxiliary state vector process can be defined, similar to the state vector process $\mathbf{Z}(t)$ in Eq. (12), as

$$\mathbf{\Xi}(t) = \begin{bmatrix} \mathbf{V}(t) \\ \dot{\mathbf{V}}(t) \end{bmatrix}_{(2n\times 1)} \tag{20}$$

Using the complex mode superposition method, the cross-covariance matrices of the state vector process $\mathbf{Z}(t)$ and auxiliary state vector process $\mathbf{\Xi}(t)$ can be obtained as

$$\mathrm{E}\left[\mathbf{Z}(t) \cdot \mathbf{Z}^T(t)\right] = \tilde{\mathbf{T}}^* \cdot \mathrm{E}\left[\mathbf{S}^*(t) \cdot \mathbf{S}^T(t)\right] \cdot \tilde{\mathbf{T}}^T \tag{21}$$

$$\mathrm{E}\left[\mathbf{Z}(t) \cdot \mathbf{\Xi}^T(t)\right] = \tilde{\mathbf{T}}^* \cdot \mathrm{E}\left[\mathbf{S}^*(t) \cdot \mathbf{\Sigma}^T(t)\right] \cdot \tilde{\mathbf{T}}^T \tag{22}$$

in which $\mathrm{E}[\ldots]$ = expectation operator; $\Sigma = [\Sigma_1(t) \Sigma_2(t) \ldots \Sigma_{2n}(t)]^T$, where

$$\Sigma_i(t) = -j \cdot \int_{-\infty}^{\infty} \mathrm{sgn}(\omega) \cdot A_{S_i}(\omega, t) \cdot e^{j\cdot\omega\cdot t} \cdot \mathrm{d}Z(\omega); \quad i = 1, 2, \ldots, 2n \tag{23}$$

Eqs. (21) and (22) show that all quantities in Eq. (18) can be computed from the following spectral characteristics of complex-valued nonstationary stochastic processes ($i, m = 1, 2, \ldots, 2n$):

$$\mathrm{E}\left[S_i^*(t) \cdot S_m(t)\right] = \sigma_{S_iS_m}(t) \tag{24}$$

$$\mathrm{E}\left[S_i^*(t) \cdot \Sigma_m(t)\right] = \sigma_{S_i\Sigma_m}(t) \tag{25}$$

Knowledge of the spectral characteristics defined in Eqs. (24) and (25) allows computation of the zeroth to second-order NGSCs of the components of any response vector $\mathbf{Q}(t)$ linearly related to the displacement response vector $\mathbf{U}(t)$ [i.e., $\mathbf{Q}(t) = \mathbf{B} \cdot \mathbf{U}(t)$, with $\mathbf{B}$ = constant matrix].

Response Statistics of MDOF Linear Systems Subjected to Fully Nonstationary Loading

A fully nonstationary process (i.e., with time-varying amplitude and frequency content) can be obtained as the superposition of component time-modulated colored noise processes (also called uniformly modulated component processes). The expression given in Eq. (16) describing a general nonstationary loading process reduces to

$$F(t) = \sum_{f=1}^{N_c} \left[A_f(t) \cdot P_f(t) \right] \tag{26}$$

in which N_c = number of component processes; $A_f(t) = f$th frequency-independent time-modulating function ($f = 1, 2, \ldots, N_c$); $P_f(t) = f$th stationary colored noise process, with PSD function having the following general expression:

$$\Phi_f(\omega) = S_{0f} \cdot \sum_{k=1}^{N_f} \sum_{l=0}^{n_k} \frac{A_{kl}}{\left(\omega - \overline{\omega}_k\right)^l} \tag{27}$$

in which A_{kl} and $\overline{\omega}_k$ ($k = 1, 2, \ldots, N_f$) = complex-valued constants; and S_{0f} = real-valued scaling constant. In this paper, it is assumed that the frequency-independent time-modulating functions $A_f(t)$ have the following general expression:

$$A_f(t) = H(t) \cdot \sum_{q=1}^{M_f} \left(a_q \cdot t^{s_q} \cdot e^{b_q \cdot t} \right) \tag{28}$$

in which a_q, b_q, and s_q ($q = 1, 2, \ldots, M_f$) = real-valued constants; and $H(t)$ = unit-step function.

Substituting Eq. (28) for $A_f(t)$ into Eq. (17) for $A_F(\omega, \tau)$, and considering only integer values for s_q ($q = 1, 2, \ldots, M_f$), yields ($i = 1, 2, \ldots, 2n$)

$$A_{S_i}(\omega, t) = \sum_{q=1}^{M_f} \left\{ a_q \cdot e^{b_q \cdot t} \cdot (s_q)! \cdot \sum_{p=0}^{s_q} \left[\frac{(-1)^p \cdot t^{(s_q - p)}}{(s_q - p)! \cdot \theta_{qi}^{(p+1)}} \right] \right\} + e^{(\lambda_i - j \cdot \omega) \cdot t} \cdot \sum_{q=1}^{M_f} \left[a_q \cdot \frac{(-1)^{(s_q+1)} \cdot (s_q)!}{\theta_{qi}^{(s_q+1)}} \right] \tag{29}$$

where $\theta_{qi} = j \cdot (\omega - \omega_{qi})$ and $\omega_{qi} = j \cdot (b_q - \lambda_i)$.

Substituting Eqs. (27) and (29) into Eq. (6) [where the embedded stationary process $X_S(\omega)$ becomes $P_f(t)$ and therefore $\Phi_{X_s X_s}(\omega) = \Phi_f(\omega)$], and the resulting expression into the first part of Eq. (4), the time-domain complex modal response statistics defined in Eq. (24) can be computed as ($i, m = 1, 2, \ldots, 2n$)

$$\begin{aligned} \sigma_{S_i S_m}(t) = \sum_{f=1}^{N_c} S_{0f} \cdot \sum_{q=1}^{M_f} \sum_{r=1}^{M_f} \sum_{k=1}^{N_f} \sum_{l=0}^{n_k} a_q \cdot a_r \cdot A_{kl} \cdot (s_q)! \cdot (s_r)! \cdot \Bigg\{ & e^{(b_q + b_r) \cdot t} \cdot \sum_{p=0}^{s_q} \sum_{u=0}^{s_r} \left[\frac{(-1)^p \cdot j^{(p+u)} \cdot t^{(s_q + s_r - p - u)}}{(s_q - p)! \cdot (s_r - u)!} \cdot I_0^{iqp,mru,l} \right] \\ & + e^{(\lambda_i^* + \lambda_m) \cdot t} \cdot (-1)^{s_q} \cdot j^{(s_q + s_r)} \cdot I_0^{iqs_q,mrs_r,l} \\ & - e^{(\lambda_i^* + b_r) \cdot t} \cdot (-j)^{s_q} \cdot \sum_{u=0}^{s_r} \left[\frac{j^u \cdot t^{(s_r - u)}}{(s_r - u)!} \cdot I_{+1}^{iqs_q,mru,l} \right] \cdot - e^{(\lambda_m + b_q) \cdot t} \cdot j^{s_r} \cdot \sum_{p=0}^{s_q} \left[\frac{(-j)^p \cdot t^{(s_q - p)}}{(s_q - p)!} \cdot I_{-1}^{iqp,mrs_r,l} \right] \Bigg\} \end{aligned} \tag{30}$$

in which

$$\begin{aligned} I_g^{iqp,mru,l} &= \int_{-\infty}^{+\infty} \frac{e^{g \cdot j \cdot \omega \cdot t} \cdot \mathrm{d}\omega}{\left(\omega - \omega_{qi}^*\right)^{(p+1)} \cdot (\omega - \omega_{rm})^{(u+1)} \cdot \left(\omega - \overline{\omega}_k\right)^l} \\ &= \sum_{s=1}^{p+1} A_s^{(g)} \cdot \int_{-\infty}^{+\infty} \frac{e^{g \cdot j \cdot \omega \cdot t} \cdot \mathrm{d}\omega}{\left(\omega - \omega_{qi}^*\right)^s} + \sum_{s=1}^{u+1} B_s^{(g)} \cdot \int_{-\infty}^{+\infty} \frac{e^{g \cdot j \cdot \omega \cdot t} \cdot \mathrm{d}\omega}{(\omega - \omega_{rm})^s} + \sum_{s=1}^{l} C_s^{(g)} \cdot \int_{-\infty}^{+\infty} \frac{e^{g \cdot j \cdot \omega \cdot t} \cdot \mathrm{d}\omega}{\left(\omega - \overline{\omega}_k\right)^s} \end{aligned} \tag{31}$$

where $A_s^{(g)}$, $B_s^{(g)}$, and $C_s^{(g)}$ = complex-valued partial fraction decomposition coefficients ($g = -1, 0, +1$). The integrals in Eq. (31) can be derived analytically using Cauchy's residue theorem (Barbato 2007; Barbato and Conte 2008) (Appendix I).

Substituting Eqs. (27) and (29) into Eq. (6), and the resulting expression into the second part of Eq. (4), the spectral characteristics in Eq. (25) are obtained as ($i, m = 1, 2, \ldots, 2n$)

$$\begin{aligned} \sigma_{S_i \Sigma_m}(t) = -j \cdot \sum_{f=1}^{N_c} S_{0f} \cdot \sum_{q=1}^{M_f} \sum_{r=1}^{M_f} \sum_{k=1}^{N_f} \sum_{l=0}^{n_k} a_q \cdot a_s \cdot A_{kl} \cdot (s_q)! \cdot (s_r)! \cdot \Bigg\{ & e^{(b_q + b_r) \cdot t} \cdot \sum_{p=0}^{s_q} \sum_{u=0}^{s_r} \left[\frac{(-1)^p \cdot j^{(p+u)} \cdot t^{(s_q + s_r - p - u)}}{(s_q - p)! \cdot (s_r - u)!} \cdot J_0^{iqp,mru,l} \right] \\ & + e^{(\lambda_i^* + \lambda_m) \cdot t} \cdot (-1)^{s_q} \cdot j^{(s_q + s_r)} \cdot J_0^{iqs_q,mrs_r,l} - e^{(\lambda_i^* + b_r) \cdot t} \cdot (-j)^{s_q} \cdot \sum_{u=0}^{s_r} \left[\frac{j^u \cdot t^{(s_r - u)}}{(s_r - u)!} \cdot J_{+1}^{iqs_q,mru,l} \right] \\ & - e^{(\lambda_m + b_q) \cdot t} \cdot j^{s_r} \cdot \sum_{p=0}^{s_q} \left[\frac{(-j)^p \cdot t^{(s_q - p)}}{(s_q - p)!} \cdot J_{-1}^{iqp,mrs_r,l} \right] \Bigg\} \end{aligned} \tag{32}$$

in which

$$J_g^{iqp,mru,l} = \int_{-\infty}^{+\infty} \frac{\operatorname{sgn}(\omega)\cdot e^{g\cdot j\cdot\omega\cdot t}\cdot \mathrm{d}\omega}{\left(\omega-\omega_{qi}^{*}\right)^{(p+1)}\cdot(\omega-\omega_{rm})^{(u+1)}\cdot(\omega-\overline{\omega}_k)^{l}}$$
$$= \sum_{s=1}^{p+1} A_s^{(g)}\cdot \int_{-\infty}^{+\infty} \frac{\operatorname{sgn}(\omega)\cdot e^{g\cdot j\cdot\omega\cdot t}\cdot \mathrm{d}\omega}{\left(\omega-\omega_{qi}^{*}\right)^{s}}$$
$$+ \sum_{s=1}^{u+1} B_s^{(g)}\cdot \int_{-\infty}^{+\infty} \frac{\operatorname{sgn}(\omega)\cdot e^{g\cdot j\cdot\omega\cdot t}\cdot \mathrm{d}\omega}{(\omega-\omega_{rm})^{s}}$$
$$+ \sum_{s=1}^{l} C_s^{(g)}\cdot \int_{-\infty}^{+\infty} \frac{\operatorname{sgn}(\omega)\cdot e^{g\cdot j\cdot\omega\cdot t}\cdot \mathrm{d}\omega}{(\omega-\overline{\omega}_k)^{s}} \tag{33}$$

can also be obtained in closed form through integration in the complex plane (Appendix II).

It is noteworthy that the input stochastic process defined by Eqs. (26)–(28) is significantly more general than the time-modulated colored noise process considered in Barbato and Vasta (2010). The solution of the integrals given in Eq. (33) is also significantly more advanced from a mathematical viewpoint than the results derived in Barbato and Vasta (2010), because of the presence of complex poles of order higher than 1. In addition, the closed-form exact solutions presented herein for the spectral characteristics of MDOF linear system response processes are valid for any kind of nonstationary excitation as described by Eqs. (26)–(28). However, the considered description of these response processes includes only first- and second-order statistical moments and, thus, is complete only for Gaussian response processes, which are generated only if the input process is Gaussian. The remainder of this paper considers nonstationary Gaussian excitations only.

First-Passage Reliability Problem for Nonstationary Response of Linear Elastic Structural Models

A classical result sought in stochastic dynamics is the failure probability for the first-passage reliability problem, referred to as first-passage failure probability (i.e., the probability that a given response quantity of an engineering system subjected to a dynamic stochastic loading out-crosses a specified threshold within a given exposure time).

A number of analytical and numerical studies have been devoted to the computation of the first-passage failure probability (Rice 1944, 1945; Crandall 1970; Corotis et al. 1972; Vanmarcke 1975; Beck 2008). However, to date, no exact closed-form solution for the first-passage failure probability is available even for the simplest case (i.e., a SDOF linear oscillator subjected to Gaussian white noise excitation with a deterministic failure threshold) (Crandall 1970; Naess 1990; Barbato and Conte 2011; Ghazizadeh et al. 2012).

Existing analytical approximations express the first-passage failure probability, $P_{f,|X|}$, for the symmetric double-barrier problem (which corresponds to the out-crossing of a failure threshold level, $x_{\lim}$, by the absolute value of the random process $X(t)$ from at-rest initial conditions) as follows:

$$P_{f,|X|}(x_{\lim},t) = 1-\exp\left[-\int_0^t h_{|X|}(x_{\lim},\tau)\cdot \mathrm{d}\tau\right] \tag{34}$$

where $h_{|X|}$ = time-variant hazard function for the symmetric double-barrier problem. The most widely used approximations are the Poisson's (P) approximation, $h_{\mathrm{P},|X|}$ (Rice 1944, 1945); the classical Vanmarcke's (cVM) approximation, $h_{\mathrm{cVM},|X|}$; and the modified Vanmarcke's (mVM) approximation, $h_{\mathrm{mVM},|X|}$ (Corotis et al. 1972; Vanmarcke 1975). The corresponding approximate time-variant hazard functions are given by

$$h_{\mathrm{P},|X|}(x_{\lim},t) = \nu_{|X|}(x_{\lim},t) \tag{35}$$

$$h_{\mathrm{cVM},|X|}(x_{\lim},t) = \nu_{|X|}(x_{\lim},t)\cdot \frac{1-\exp\left[-\sqrt{\pi/2}\cdot q_X(t)\cdot \frac{x_{\lim}}{\sigma_X(t)}\right]}{1-\exp\left\{-\frac{1}{2}\cdot\left[\frac{x_{\lim}}{\sigma_X(t)}\right]^2\right\}} \tag{36}$$

$$h_{\mathrm{mVM},|X|}(x_{\lim},t) = \nu_{|X|}(x_{\lim},t)\cdot \frac{1-\exp\left\{-\sqrt{\pi/2}\cdot[q_X(t)]^{1.2}\cdot \frac{x_{\lim}}{\sigma_X(t)}\right\}}{1-\exp\left\{-\frac{1}{2}\cdot\left[\frac{x_{\lim}}{\sigma_X(t)}\right]^2\right\}} \tag{37}$$

in which $\nu_{|X|}$ = mean out-crossing rate of process $X(t)$; $\sigma_X(t)$ = SD function of process $X(t)$; and $q_X(t)$ = bandwidth parameter function of process $X(t)$.

Application Example

This paper presents as an application example a linear shear-type MDOF model of a 3-story building subjected to a nonstationary base excitation defined by a fully nonstationary stochastic earthquake ground motion model (Conte and Peng 1997). This stochastic base excitation model was calibrated to reproduce the statistical characteristics of the N90W (W-E) component of the Loma Prieta earthquake of October 17, 1989, recorded at the Capitola site (referred to as the Capitola earthquake record in the remainder of the paper).

Stochastic Base Excitation Model

The Conte and Peng (1997) stochastic earthquake ground motion model, $\ddot{U}_g(t)$, is defined as the sum of a finite number of pairwise statistically independent, uniformly modulated Gaussian processes

$$\ddot{U}_g(t) = \sum_{f=1}^{N_f}\left[A_f(t)\cdot Q_f(t)\right] \tag{38}$$

where $Q_f(t)$ = fth Gaussian stationary subcomponent process with PSD function defined as

$$\Phi_{Q_fQ_f}(\omega) = \frac{\nu_f\cdot S_{0f}}{2\cdot\pi}\cdot\left[\frac{1}{\nu_f^2+(\omega+\eta_f)^2}+\frac{1}{\nu_f^2+(\omega-\eta_f)^2}\right]$$
$$= \frac{j\cdot S_{0f}}{4\cdot\pi}\cdot\sum_{k=1}^{4}\left[\frac{(-1)^k}{(\omega-\tilde{\omega}_{fk})}\right] \tag{39}$$

in which η_f, ν_f = PSD shape parameters; $\tilde{\omega}_{f1}=-\tilde{\omega}_{f4}=-\eta_f+j\cdot\nu_f$ and $\tilde{\omega}_{f2}=-\tilde{\omega}_{f3}=-\eta_f-j\cdot\nu_f$; and $A_f(t)$ = time-modulating function defined as

$$A_f(t) = \alpha_f \cdot (t - \theta_f)^{\beta_f} \cdot e^{-\gamma_f \cdot (t-\theta_f)} \cdot H(t - \theta_f) \quad (40)$$

where $\alpha_f, \beta_f, \gamma_f, \theta_f$ = parameters obtained by fitting the stochastic ground motion model to a given historical earthquake record.

The parameters of the earthquake ground motion model fitted to the Capitola earthquake record are given in Table 1. Fig. 1 shows the evolutionary PSD function of the Capitola earthquake ground motion model.

Linear MDOF Structural Model

The 3-story, 1-bay, steel, shear-type frame considered in this application example is shown in Fig. 2. This building structure has a uniform story height $H = 3.20$ m and a bay width $L = 6.00$ m. The steel columns, made of European HE340A wide-flange beams with moment of inertia along the strong axis $I = 27{,}690.0$ cm^4, were assumed inextensible. The steel material was modeled as linear elastic with Young's modulus $E = 200$ GPa. The beams were considered to be rigid to enforce a typical shear building behavior. Under these assumptions, the shear frame was modeled as a three-DOF linear system.

The frame thus described was assumed to be part of a building structure with a distance between frames $L' = 6.00$ m. The tributary mass per story, M, was obtained assuming a distributed gravity load of $w = 8$ kN/m^2, accounting for the structure's self-weight, as well as for permanent and live loads, and is equal to $M = 28{,}800$ kg. The modal periods of the linear elastic undamped shear frame are $T_1 = 0.38$, $T_2 = 0.13$, and $T_3 = 0.09$ s, with corresponding effective modal mass ratios of 91.4, 7.5, and 1.1%, respectively. Viscous damping in the form of Rayleigh damping was assumed, with a damping ratio $\xi = 0.02$ for the first and third modes of vibration. The second mode had a damping ratio of 0.017. The same shear frame was also considered with the addition of a viscous damper with coefficient $c = 200$ kN · s/m across the first story, as shown in Fig. 2. The structure with a viscous damper is a nonclassically damped system with first-, second-, and third-mode damping ratios of 0.037, 0.048, and 0.034, respectively.

Table 1. Parameters of Ground Acceleration Model for Capitola Earthquake

f	α_f (cm/s$^{2+\beta}$)	β_f	γ_f (1/s)	θ_f (s)	ν_f (rad/s)	η_f (rad/s)
1	5×10^{-4}	20	3.4695	2.71	0.243	9.342
2	44.47	6	1.4969	10.68	0.807	7.728
3	3.43	6	1.2859	18.13	1.331	5.675
4	3×10^{-4}	16	2.2607	−0.21	2.559	15.461
5	0.11	8	1.2017	6.02	2.079	18.367
6	3.09	6	1.0599	0.26	2.105	29.731
7	21.75	6	2.1355	11.67	0.229	21.770
8	4.86	6	1.0942	−0.47	2.272	39.640
9	4.67	8	1.6931	−0.11	1.560	46.113
10	15.49	8	2.0498	0.80	1.960	51.334
11	0.46	8	1.3538	−0.40	8.208	59.656

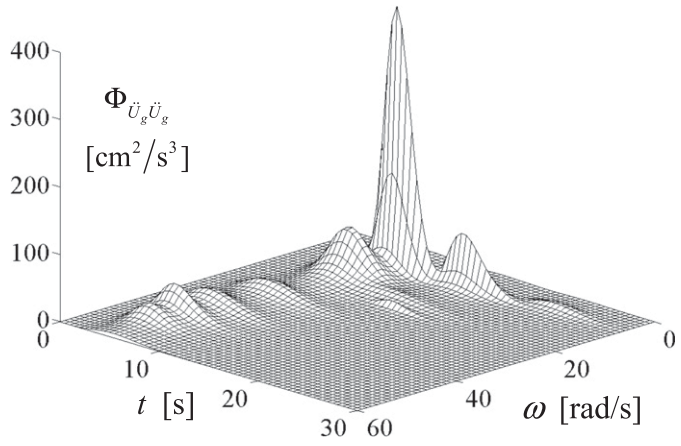

Fig. 1. Evolutionary PSD function of ground acceleration model for Capitola earthquake

Spectral Characteristics of the Displacement and Velocity Responses Relative to the Ground

Figs. 3 and 4 show the time histories of the SDs of the floor displacements relative to the ground (in short, relative displacements) for the classically damped (i.e., without viscous damper) and the nonclassically damped (i.e., with viscous damper) structure, respectively. Figs. 5 and 6 show the time histories of the SDs of the floor velocities relative to the ground (in short, relative velocities) for the classically damped and the nonclassically damped structure, respectively. In the nonclassically damped case, as compared with

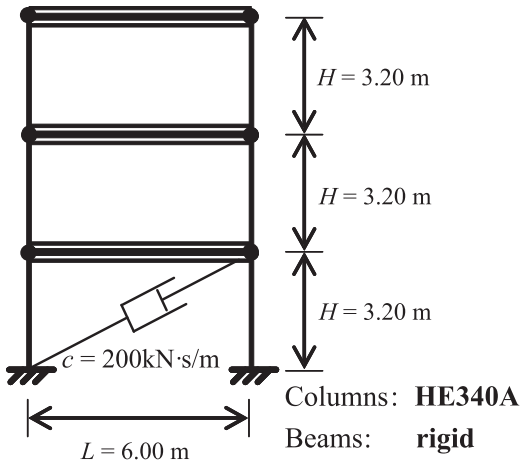

Fig. 2. Geometric configuration of benchmark 3-story, 1-bay, shear-type steel frame

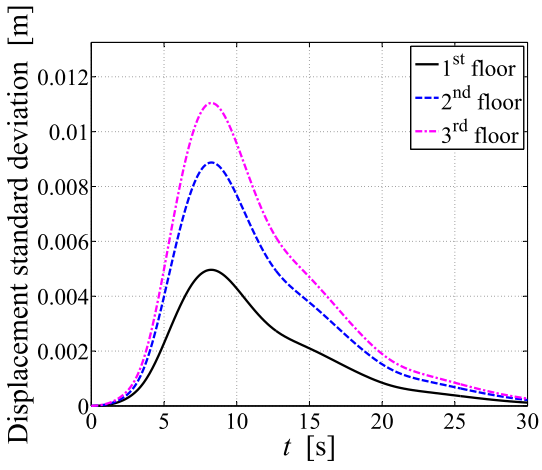

Fig. 3. SDs of floor relative displacements for classically damped structure

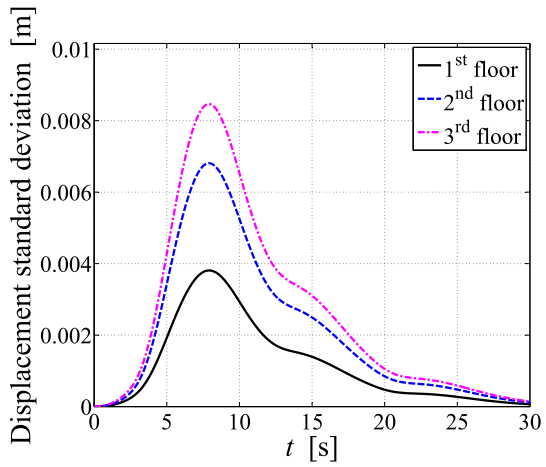

Fig. 4. SDs of floor relative displacements for nonclassically damped structure

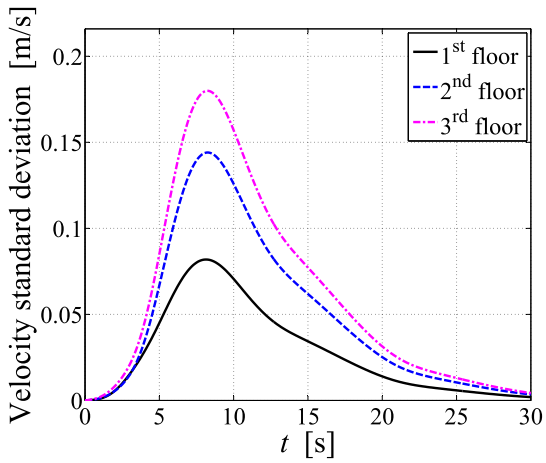

Fig. 5. SDs of floor relative velocities for classically damped structure

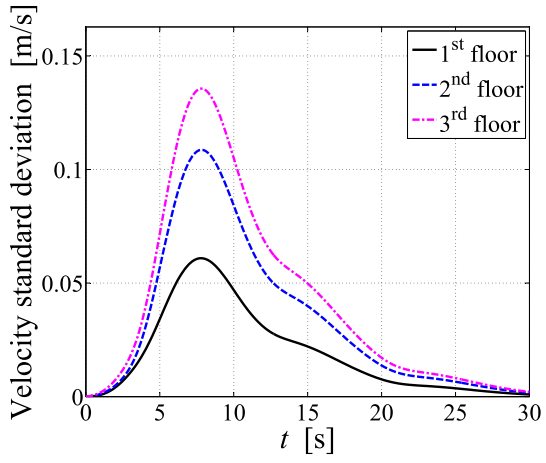

Fig. 6. SDs of floor relative velocities for nonclassically damped structure

the classically damped case, it is observed that (1) the peak values of both the relative displacement and the velocity SDs reduce significantly, (2) the peak values of these SDs are reached slightly earlier, and (3) all SD time histories have a very similar shape.

Figs. 7 and 8 show the time histories of the bandwidth parameters of the floor relative displacement responses (in short, bandwidth parameters) for the classically damped and the nonclassically damped structure, respectively. The following observations are made. (1) The values of the bandwidth parameters change significantly over the earthquake duration and are lowest in the time period between 5 and 20 s from the start of the seismic excitation. This time period corresponds to the period in which the seismic excitation is the most intense and the displacement responses are largest. During this strong ground motion phase, the response is controlled mainly by the first mode of vibration of the structure. (2) The values of the bandwidth parameters for the nonclassically damped structure become increasingly larger than their counterparts for the classically damped structure, particularly for $t > 10$ s. (3) The bandwidth parameter of the first floor relative displacement is always larger than the bandwidth parameters of the second and third floors, for both the classically and nonclassically damped structure. (4) The time histories of the bandwidth parameters of the second and third floor relative displacements almost coincide, for both the classically and nonclassically damped structure.

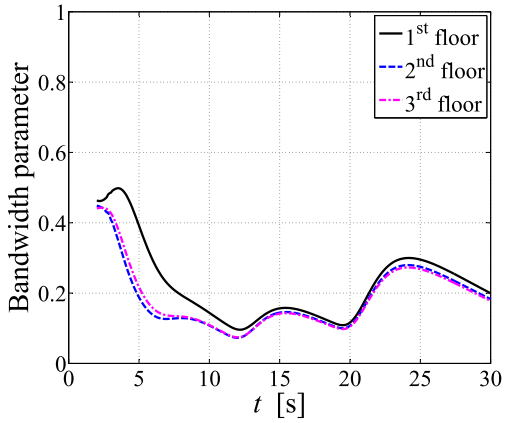

Fig. 7. Bandwidth parameters of floor relative displacements for classically damped structure

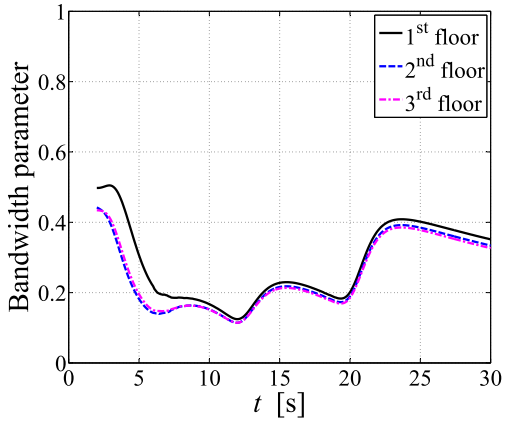

Fig. 8. Bandwidth parameters of floor relative displacements for nonclassically damped structure

Figs. 9 and 10 show the time histories of the central frequencies normalized by the first-mode natural frequency (in short, normalized central frequencies) of the floor relative displacement responses for the classically and the nonclassically damped structure, respectively. It is observed that (1) the values of the normalized central frequencies are slightly lower for the nonclassically damped structure than for the classically damped structure; and (2) the normalized central frequencies are very close to unity in the time interval of 5–20 s, which corresponds to the strong-motion phase of the seismic excitation. This latter observation confirms that the structural response is dominated by the structure's first mode of vibration, particularly during the strong ground motion phase.

The results presented in Figs. 7–10 (i.e., time histories of the bandwidth parameters and normalized central frequencies of the floor relative displacements) do not include the first 2 s of the time histories. In fact, during the first 2 s of seismic excitation, the values of the spectral characteristics [i.e., $\sigma^2_{U_i}(t)$, $\sigma^2_{\dot{U}_i}(t)$, $\sigma_{U_i\dot{U}_i}(t)$, and $\sigma_{U_i\dot{V}_i}(t)$] are very small (of the order of the machine precision when using double-precision numbers). Thus, the values of the central frequencies and bandwidth parameters computed using Eqs. (8) and (9), respectively, are inaccurate during the first 2 s of the time histories because of round-off errors deriving from the use of finite-precision arithmetic. All closed-form solutions presented in this paper were verified through comparison with Monte Carlo simulation results.

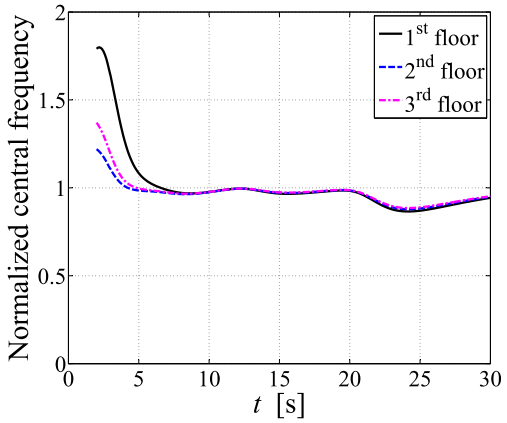

Fig. 9. Normalized central frequencies of floor relative displacements for classically damped structure

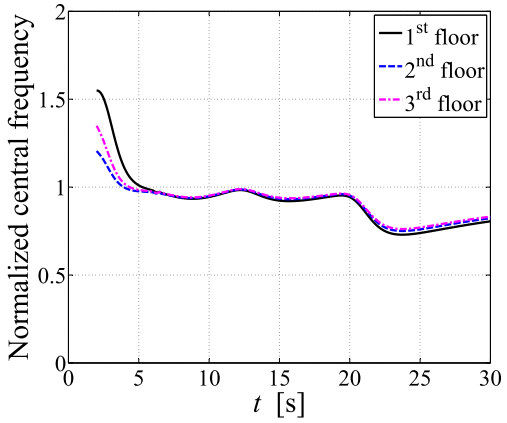

Fig. 10. Normalized central frequencies of floor relative displacements for nonclassically damped structure

First-Passage Failure Probability Estimates

The analytical approximations of the hazard function given in Eqs. (35)–(37) (i.e., P, cVM, and mVM approximations) were used to estimate the time-variant failure probability $P_{f,|U_{\text{roof}}|}$ corresponding to the relative displacement of the roof with respect to the ground, U_{roof}, out-crossing a specified deterministic threshold, U_{lim}. In this example, both the classically and the nonclassically damped structural models were considered in combination with two values of U_{lim} (i.e., $U_{\text{lim}} = 0.003 \cdot H_{\text{tot}} = 0.0288$ m and $U_{\text{lim}} = 0.004 \cdot H_{\text{tot}} = 0.0384$ m, where $H_{\text{tot}} = 9.2$ m = total height of the building). The analytical estimates of $P_{f,|U_{\text{roof}}|}$ were compared with the corresponding numerical estimates obtained using Monte Carlo simulation. The earthquake ground motion realizations for the Monte Carlo simulation analysis were simulated using the method described in Barbato and Conte (2009), and the time histories of the structural responses of interest were obtained using the exact integration method for piecewise linear excitations (Chopra 2001). In addition, the SD of the Monte Carlo estimate of the failure probability was estimated and is shown as an error band (i.e., mean ± SD) in Figs. 11–14. For the sake of clarity, the first-passage failure probability results presented in Figs. 11–14 are shown for the time interval of 5–15 s, which corresponds to the strong-motion phase of

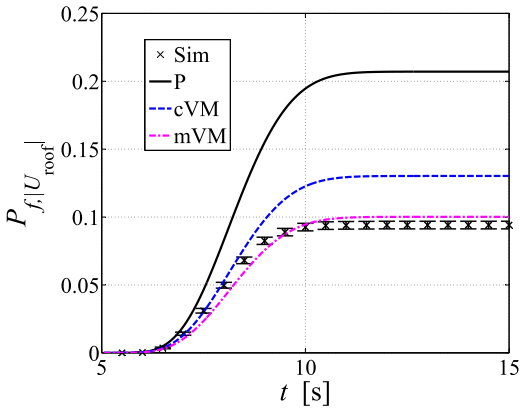

Fig. 11. Failure probability for classically damped structure ($U_{\text{lim}} = 0.003 \cdot H_{\text{tot}}$)

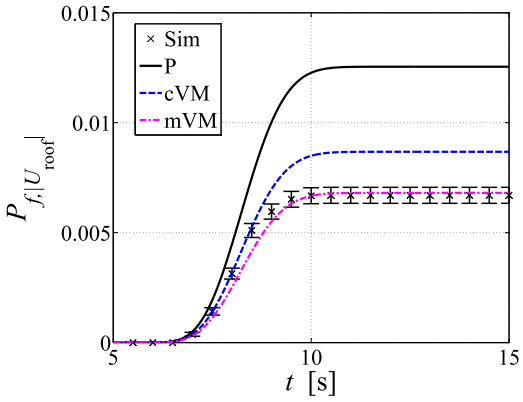

Fig. 12. Failure probability for classically damped structure ($U_{\text{lim}} = 0.004 \cdot H_{\text{tot}}$)

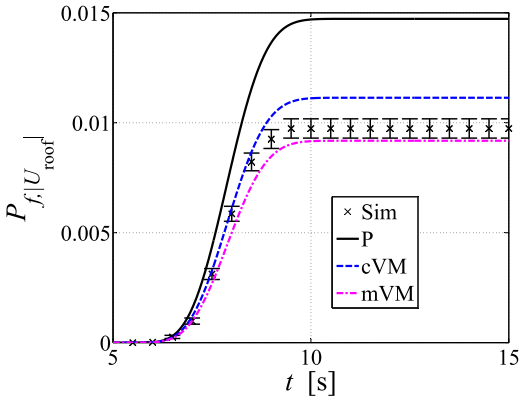

Fig. 13. Failure probability for nonclassically damped structure ($U_{lim} = 0.003 \cdot H_{tot}$)

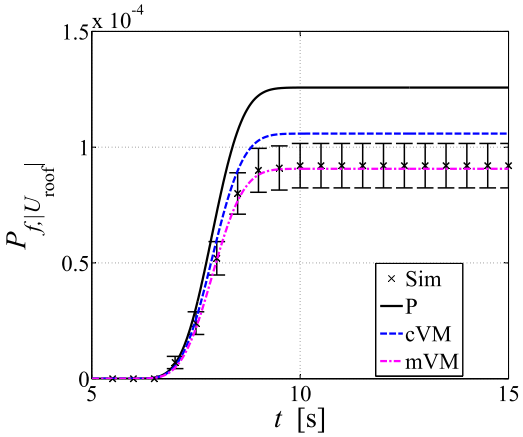

Fig. 14. Failure probability for nonclassically damped structure ($U_{lim} = 0.004 \cdot H_{tot}$)

the earthquake ground motion. In fact, the estimated changes in failure probabilities are negligible outside this time interval.

Figs. 11–14 compare the P, cVM, and mVM approximations of the time-variant failure probability with the corresponding Monte Carlo simulation estimates (denoted as Sim in the figures) for the classically (Figs. 11 and 12) and the nonclassically (Figs. 13 and 14) damped structural models, and for roof displacement thresholds $U_{lim} = 0.003 \cdot H_{tot}$ (Figs. 11 and 13) and $U_{lim} = 0.004 \cdot H_{tot}$ (Figs. 12 and 14). The Monte Carlo simulation results are based on 10,000 time history realizations for the classically damped structure with $U_{lim} = 0.003 \cdot H_{tot}$ (Fig. 11), 50,000 time history realizations for the classically damped structure with $U_{lim} = 0.004 \cdot H_{tot}$ (Fig. 12) and for the nonclassically damped structure with $U_{lim} = 0.003 \cdot H_{tot}$ (Fig. 13), and 1,000,000 time history realizations for the nonclassically damped structure with $U_{lim} = 0.004 \cdot H_{tot}$ (Fig. 14).

Based on the results presented in Figs. 11–14, the following observations are made: (1) the P approximation always overestimates (often significantly) the Monte Carlo simulation results, with the relative error decreasing as the probability of failure decreases; (2) among the three analytical approximations, the cVM approximation is the closest to the Monte Carlo simulation results in the time window of 6.5–8.5 s in which the largest rate of change of $P_{f,|U_{roof}|}$ is observed, whereas it generally overestimates the final value of the failure probability; and (3) the mVM analytical approximation provides results that are generally close to the Monte Carlo simulation results, especially for the final value of the failure probability. The Monte Carlo simulation results are very accurate for the classically damped structure with $U_{lim} = 0.003 \cdot H_{tot}$, as shown by the narrow width of the mean ± 1 SD error band relative to the failure probability values (Fig. 11). The final value of the failure probability estimate obtained using Monte Carlo simulation for the classically damped structure is more than 10 times smaller when $U_{lim} = 0.004 \cdot H_{tot}$ than when $U_{lim} = 0.003 \cdot H_{tot}$. The final value of the Monte Carlo simulation estimate of the failure probability for the nonclassically damped structure is more than 100 times smaller when $U_{lim} = 0.004 \cdot H_{tot}$ than when $U_{lim} = 0.003 \cdot H_{tot}$. In addition, the Monte Carlo estimate of the final value of the failure probability is about 10 times smaller for the nonclassically damped structure than the corresponding estimate for the classically damped structure for $U_{lim} = 0.003 \cdot H_{tot}$, and about 100 times smaller for $U_{lim} = 0.004 \cdot H_{tot}$, which shows that the use of viscous dampers is an effective retrofit method to reduce the roof drift of the considered structure. Finally, by comparing the results presented in Figs. 11–14, it is observed that the differences in the failure probability estimates obtained using the three analytical approximations considered in this study become smaller for decreasing values of the failure probability.

Conclusions

In this paper, complex modal analysis and complex plane integration were used to derive new closed-form analytical solutions for the NGSCs of nonstationary stochastic processes representing the response of linear elastic structural models subjected to fully nonstationary earthquake ground motion processes. These newly derived closed-form solutions were used to derive closed-form solutions for the time-variant bandwidth parameter and central frequency, and analytical approximations of the failure probability (based on the maximum roof displacement response) for linear elastic MDOF structural models subjected to seismic base excitation represented by a well-known fully nonstationary earthquake ground motion model. The new analytical results presented in this paper can be used (1) as benchmark solutions for the validation of numerical methods of stochastic dynamics in the linear elastic range of structural behavior, (2) in probabilistic seismic loss analysis of nonstructural components and systems in building structures subjected to moderate earthquakes, and (3) in structural engineering applications requiring a fast estimate of the failure probability for linear elastic systems.

Appendix I. Computation of Integrals in Eq. (31)

$$\int_{-\infty}^{+\infty} \frac{e^{g \cdot j \cdot \omega \cdot t} \cdot d\omega}{(\omega - \tilde{\omega})^s} = \frac{2 \cdot g \cdot j \cdot \pi}{(s-1)!} \cdot e^{g \cdot j \cdot \omega \cdot t} \cdot (g \cdot j \cdot t)^{(s-1)} \cdot \left\langle \frac{g \cdot \mathrm{Im}(\tilde{\omega})}{|\mathrm{Im}(\tilde{\omega})|} \right\rangle, \quad (g = -1, +1) \tag{41}$$

$$\int_{-\infty}^{+\infty} \frac{d\omega}{(\omega - \tilde{\omega})^s} = \begin{cases} 2 \cdot \pi \cdot j \cdot \left\langle \dfrac{\mathrm{Im}(\tilde{\omega})}{|\mathrm{Im}(\tilde{\omega})|} \right\rangle & (g = 0, s = 1) \\ 0 & (g = 0,\ s > 1) \end{cases} \tag{42}$$

in which $\tilde{\omega}$ = complex-valued constant; Im(...) = imaginary part of the quantity in parentheses; and $\langle \ldots \rangle$ = Macaulay brackets (defined so that $\langle x \rangle = 0$ if $x < 0$ and $\langle x \rangle = x$ if $x \geq 0$).

Appendix II. Computation of Integrals in Eq. (33)

$$\int_{-\infty}^{+\infty} \frac{\text{sgn}(\omega)\cdot e^{g\cdot j\cdot\omega\cdot t}\cdot d\omega}{(\omega-\tilde{\omega})^s} = 2\cdot e^{g\cdot j\cdot\omega\cdot t}\cdot (g\cdot j\cdot t)^{(s-1)}\cdot \left\{ \begin{array}{c} \dfrac{g\cdot j\cdot\pi}{(s-1)!}\cdot \text{sgn}[\text{Re}(\tilde{\omega})]\cdot \left\langle \dfrac{g\cdot \text{Im}(\tilde{\omega})}{|\text{Im}(\tilde{\omega})|}\right\rangle \\ +(-1)^{(s-1)}\cdot \Gamma(1-s, g\cdot j\cdot\tilde{\omega}\cdot t) \end{array} \right\}, \quad (g=-1,\ +1) \tag{43}$$

$$\int_{-\infty}^{+\infty} \frac{\text{sgn}(\omega)\cdot d\omega}{(\omega-\tilde{\omega})^s} = 2\cdot \frac{(-1)^{(s-1)}}{s-1}\cdot \tilde{\omega}^{(1-s)}, \quad (g=0,\ s>1) \tag{44}$$

$$\begin{aligned} A_1^{(g)}\cdot \int_{-\infty}^{+\infty} \frac{\text{sgn}(\omega)\cdot d\omega}{\omega-\omega_{qi}^*} + B_1^{(g)}\cdot \int_{-\infty}^{+\infty} \frac{\text{sgn}(\omega)\cdot d\omega}{\omega-\omega_{rm}} \\ + C_1^{(g)}\cdot \int_{-\infty}^{+\infty} \frac{\text{sgn}(\omega)\cdot d\omega}{\omega-\overline{\omega}_k} = -2\cdot \Big[A_1^{(g)}\cdot \log\left(-\omega_{qi}^*\right) \\ + B_1^{(g)}\cdot \log(-\omega_{rm}) + C_1^{(g)}\cdot \log(-\overline{\omega}_k)\Big], \quad (g=0, s=1) \end{aligned} \tag{45}$$

in which $\text{Re}(\ldots)$ = real part of the quantity in parentheses; $\Gamma(\ldots,\ldots)$ = incomplete Gamma function (Abramowitz and Stegun 1972a, b); and $\log(\ldots)$ = principal value of the complex logarithm (with branch cut along the negative real axis).

Acknowledgments

Partial support of this research by (1) the Longwell's Family Foundation through the Fund for Innovation in Engineering Research (FIER) Program, (2) the Louisiana State University Council on Research through the 2009-2010 Faculty Research Grant Program, and (3) the Louisiana Board of Regents (LA BoR) through the Louisiana Board of Regents Research and Development Program, Research Competitiveness (RCS) subprogram under Award No. LESQSF(2010-13)-RD-A-01, is gratefully acknowledged. Any opinions, findings, conclusions or recommendations expressed in this publication are those of the authors and do not necessarily reflect the views of the sponsoring agencies.

References

Abramowitz, M., and Stegun, I. A. (1972a). "Exponential integral and related functions." Chapter 5, *Handbook of mathematical functions with formulas, graphs, and mathematical tables*, Dover, New York, 227–251.

Abramowitz, M., and Stegun, I. A. (1972b). "Gamma function and related functions." Chapter 6, *Handbook of mathematical functions with formulas, graphs, and mathematical tables*, Dover, New York, 253–293.

Arens, R. (1957). "Complex processes for envelopes of normal noise." *IRE Trans. Inf. Theory*, 3(3), 204–207.

Barbato, M. (2007). "Finite element response sensitivity, probabilistic response and reliability analyses of structural systems with applications to earthquake engineering." Ph.D. dissertation, Dept. of Structural Engineering, Univ. of California, San Diego, La Jolla, CA.

Barbato, M., and Conte, J. P. (2008). "Spectral characteristics of non-stationary random processes: Theory and applications to linear structural models." *Probab. Eng. Mech.*, 23(4), 416–426.

Barbato, M., and Conte, J. P. (2009). "New efficient simulation technique for fully non-stationary stochastic earthquake ground motion." *Proc., 10th Int. Conf. on Structural Safety and Reliability (ICOSSAR): Safety, Reliability and Risk of Structures, Infrastructures and Engineering Systems*, H. Furuta, D. M. Frangopol, and M. Shinozuka, eds., Taylor & Francis, London, 1676–1682.

Barbato, M., and Conte, J. P. (2011). "Structural reliability applications of nonstationary spectral characteristics." *J. Eng. Mech.*, 10.1061/(ASCE)EM.1943-7889.0000238, 371–382.

Barbato, M., and Vasta, M. (2010). "Closed-form solutions for the time-variant spectral characteristics of non-stationary random processes." *Probab. Eng. Mech.*, 25(1), 9–17.

Beck, A. T. (2008). "The random barrier-crossing problem." *Probab. Eng. Mech.*, 23(2–3), 134–145.

Chopra, A. K. (2001). *Dynamics of structures: Theory and applications to earthquake engineering*, 2nd Ed., Prentice Hall, Englewood Cliffs, NJ.

Conte, J. P., and Peng, B. F. (1997). "Fully nonstationary analytical earthquake ground-motion model." *J. Eng. Mech.*, 10.1061/(ASCE)0733-9399(1997)123:1(15), 15–24.

Corotis, R. B., Vanmarcke, E. H., and Cornell, A. C. (1972). "First passage of nonstationary random processes." *J. Engrg. Mech. Div.*, 98(2), 401–414.

Crandall, S. H. (1970). "First-crossing probabilities of the linear oscillator." *J. Sound Vib.*, 12(3), 285–299.

Di Paola, M. (1985). "Transient spectral moments of linear systems." *Solid Mech. Arch.*, 10, 225–243.

Dugundji, J. (1958). "Envelopes and pre-envelopes of real waveforms." *IRE Trans. Inf. Theory*, 4(1), 53–57.

Ghazizadeh, S., Barbato, M., and Tubaldi, E. (2012). "New analytical solution of the first-passage reliability problem for linear oscillators." *J. Eng. Mech.*, 10.1061/(ASCE)EM.1943-7889.0000365, 695–706.

Lin, Y. K. (1967). *Probabilistic theory of structural dynamics*, McGraw Hill, New York.

Michaelov, G., Sarkani, S., and Lutes, L. D. (1999). "Spectral characteristics of nonstationary random processes—A critical review." *Struct. Saf.*, 21(3), 223–244.

Naess, A. (1990). "Approximate first-passage and extremes of narrow-band Gaussian and non-Gaussian random vibrations." *J. Sound Vib.*, 138(3), 365–380.

Peng, B.-F., and Conte, J. P. (1998). "Closed-form solutions for the response of linear systems to fully nonstationary earthquake excitation." *J. Eng. Mech.*, 10.1061/(ASCE)0733-9399(1998)124:6(684), 684–694.

Priestley, M. B. (1965). "Evolutionary spectra and non-stationary processes." *J. R. Stat. Soc. Ser. B*, 27(2), 204–237.

Priestley, M. B. (1987). *Spectral analysis and time series, univariate series, multivariate series, prediction and control*, Academic Press, London.

Reid, J. G. (1983). *Linear system fundamentals: Continuous and discrete, classic and modern*, McGraw Hill, New York.

Rice, S. O. (1944). "Mathematical analysis of random noise." *Bell Syst. Tech. J.*, 23(3), 282–332.

Rice, S. O. (1945). "Mathematical analysis of random noise." *Bell Syst. Tech. J.*, 24(1), 46–156.

Shinozuka, M. (1970). "Random processes with evolutionary power." *J. Engrg. Mech. Div.*, 96(4), 543–545.

Spanos, P. D., and Miller, S. M. (1994). "Hilbert transform generalization of a classical random vibration integral." *J. Appl. Mech.*, 61(3), 575–581.

Spanos, P.-T. D. (1983). "Spectral moments calculation of linear system output." *J. Appl. Mech.*, 50(4a), 901–903.

Vanmarcke, E. H. (1975). "On the distribution of the first-passage time for normal stationary random processes." *J. Appl. Mech.*, 42(1), 215–220.